

## Numerical Method for the Simulation of Front Evolving Fibre Suspension Flow Using Level Set Method

H.-S. Dou<sup>1</sup>, N. Phan-Thien<sup>1</sup>, B. C. Khoo<sup>1</sup>, K. S. Yeo<sup>1</sup>, R. Zheng<sup>2</sup>

<sup>1</sup>Fluid Mechanics Division, Department of Mechanical Engineering  
National University of Singapore, Singapore 119260, SINGAPORE

<sup>2</sup>Moldflow Pty. Ltd, 259-261 Colchester Road, Kilsyth, Vic 3137, Australia

### Abstract

Numerical method for simulating the front evolution of fibre suspension flow is developed using projection and level set methods. The semi-dilute suspensions of short fibres in Newtonian fluids are considered. The governing equation for the fibre motion is the Jeffery equation and that for velocity field is the Navier-Stokes equation. The velocity field is solved using the projection method with finite difference scheme, and the fibre equations are solved with the Runge-Kutta method. Flows with two groups of parameters of semi-dilute suspension flows are simulated in a duct. These results are compared with those of Newtonian flows. It is shown that the numerical method is able to deal with the complexity due to fibre effects and to track the front of the flow. Because the fibre orientation in the flow and the shape of the flow front are of great significance to the quality of the product, this study has wide background of engineering applications.

**Keywords:** Level set; Projection; Fibre suspension; Semi-dilute; Simulation; Front flow.

### Introduction

Simulation of fibre suspensions can be used in the injecting moulding technique to improve the product quality. The quality of simulation of fibre suspension depends upon the appropriate description of the constitutive equations to the fibre properties in the flows and the correct prediction of property of the fibre flows. In the past years, several micro-structural models have been proposed for dilute suspensions and various numerical methods have been developed [1-5]. Generally, most simulations in the literature use a traditionally continuous mechanics method to solve the Navier-Stokes equations, and the contribution of the fibre motion is included in the stress terms. There are currently three kinds of numerical methods for stress contribution from the fibre suspension. One is using the assumption that the fibre is in full-alignment along with the velocity vector [6]. The second method solves the stress tensor in the flow field, and the fibre stress is modelled by a constitutive equation of the fibre orientation tensor [2,7]. The third method is that the orientation tensor of fibre is modelled by Brownian configuration field method [4,8]. Azaiez and Gulδ'nt [9] compared the fibre aligned-assumption and the solution of orientation tensors which is defined as dyadic products of the orientation vector through their FEM solution for contract problem. Their results show that the coupling between the flow and the fibre orientation is very important in the modelling.

The level set method has been developed and used in the tracing of the flow front evolution, and it demonstrated to be very useful and convenient [10,11]. However, it has not been yet applied to the fibre suspension flows. We have used this method for simulating the film flows of shear thinning flows on an inclined plates [12]. In this paper, Numerical method for simulating the front evolution of fibre suspension flow is developed using projection and level set methods. The semi-dilute suspensions of short fibres in Newtonian fluids are

considered. The Brownian configuration field method in [4,8] is employed to solve the fibre motion and their contributions. The purpose of the study is to study the effect of fibre behaviour on the front shape because it strongly influences the quality of the moulding products. Computation examples are given and the result is discussed.

### Governing Equations

The conservations of mass and momentum for an isothermal flow of fibre suspension can be expressed with the following equations,

$$\nabla \cdot \mathbf{u} = 0, \quad \rho \left( \frac{\partial \mathbf{u}}{\partial t} + \mathbf{u} \cdot \nabla \mathbf{u} \right) = -\nabla p + \nabla \cdot \boldsymbol{\tau}_f + \mu_N \nabla^2 \mathbf{u} + \rho \mathbf{g}, \quad (1)$$

where  $\rho$  is the fluid density,  $\mathbf{g}$  the gravity acceleration,  $t$  the time,  $\mathbf{u}$  the velocity vector,  $p$  the hydrodynamic pressure, and  $\boldsymbol{\tau}_f$  the stress tensor from the fibre suspension, and  $\mu_N \nabla^2 \mathbf{u}$  the stress tensor from the Newtonian fluid with  $\mu_N$  being the fluid viscosity.

The constitutive equation for the fibre stress is [3,4],

$$\boldsymbol{\tau}_f = \eta_N f(\varphi) [A \dot{\boldsymbol{\gamma}} : \langle \mathbf{p}\mathbf{p}\mathbf{p}\mathbf{p} \rangle + 2D_r F \langle \mathbf{p}\mathbf{p} \rangle], \quad (2)$$

with

$$f(\varphi) = \frac{\varphi(2 - \varphi/\varphi_m)}{2(1 - \varphi/\varphi_m)^2}, \quad A = \frac{a_r^2}{2(\ln 2a_r - 1.5)}, \quad F = \frac{3a_r^2}{\ln(2a_r - 0.5)}, \quad (3)$$

where  $\dot{\boldsymbol{\gamma}} = (\nabla \mathbf{u}^T + \nabla \mathbf{u})/2$  is the rate-of-strain tensor,  $\mathbf{p}$  a unit vector along the axis of the fibre,  $D_r$  the diffusion coefficient,  $\langle \dots \rangle$  denotes the ensemble average over the orientation space of fibres,  $\langle \mathbf{p}\mathbf{p} \rangle$  and  $\langle \mathbf{p}\mathbf{p}\mathbf{p}\mathbf{p} \rangle$  are the second and fourth-order structure tensors, respectively, and  $\varphi$  the volume concentration. The parameter  $\varphi_m$  express the maximum volume packing of fibres, and it can be approximated by the following empirical linear function of the aspect ratio,

$$\varphi_m = 0.53 - 0.013a_r, \quad 5 < a_r < 30. \quad (4)$$

In Eq.(2), the first term on the right hand side expresses the stress contribution from the fibre motion, rotation and interactions (dissipative), and the second term represents the stress contribution due to the momentum transport caused by random motion of fibres (entropic). Generally, the first term plays a dominating role over the second term.

The second and fourth order structure tensors of fibres in Eq.(2) have to be calculated after the unit vector  $\mathbf{p}$  is solved for each fibre. The evolution of the unit vector  $\mathbf{p}$  is expressed by the Jeffery equation [13],

$$\frac{d}{dt} \mathbf{p}(i) = \mathbf{L} \cdot \mathbf{p}(i) - \mathbf{L} : \mathbf{p}(i)\mathbf{p}(i)\mathbf{p}(i) + (\mathbf{I} - \mathbf{p}(i)\mathbf{p}(i)) \cdot \mathbf{F}^{(b)}(t). \quad (5)$$

Here, a diffusion term has been added to Jeffery equation according to Folgar-Tucker [1]. In Eq.(5),  $\mathbf{p}(i)$  is the unit vector along the axis of the  $i$ th fibre,  $\mathbf{L}$  the effective velocity tensor,

$\mathbf{L} = \nabla \mathbf{u}^T - \zeta \dot{\gamma}$ , with  $\zeta = (a_r + 1)^{-1}$ .  $\mathbf{F}^{(b)}(t)$  is a random force, with properties

$$\langle \mathbf{F}^{(b)}(t) \rangle = 0, \quad (6)$$

and

$$\langle \mathbf{F}^{(b)}(t+s) \mathbf{F}^{(b)}(t) \rangle = 2D_r \delta(s) \mathbf{I}, \quad (7)$$

where  $\delta(s)$  is the Dirac delta function and  $\mathbf{I}$  the unit tensor.  $D_r$  is a diffusion factor mentioned in Eq.(2). Folgar and Tucker assumed that

$$D_r = C_i \dot{\gamma}, \quad (8)$$

where  $\dot{\gamma} = \sqrt{\text{tr} \dot{\gamma}^2} / 2$  is the generalized strain rate,  $C_i$  is the interaction factor, which may be a function of  $\phi$  and  $a_r$ . Phan-Thien et al. have given a correlation of a semi empirical equation [14]. The random force can be expressed in terms of the white noise,

$$\mathbf{F}^{(b)}(t) = \sqrt{2C_i \dot{\gamma}} \frac{d\mathbf{w}_t}{dt}, \quad (9)$$

where  $\mathbf{w}_t$  is the Wiener process and it is a Gaussian random function.

After the Eq.(5) for  $\mathbf{p}(i)$  is solved, one can calculate the structure tensor using the ensemble average:

$$\langle \mathbf{p}\mathbf{p} \rangle = \frac{1}{N} \sum_{i=1}^N \mathbf{p}(i) \mathbf{p}(i), \quad \langle \mathbf{p}\mathbf{p}\mathbf{p}\mathbf{p} \rangle = \frac{1}{N} \sum_{i=1}^N \mathbf{p}(i) \mathbf{p}(i) \mathbf{p}(i) \mathbf{p}(i), \quad (10)$$

where  $N$  is the number of fibres. Now, introducing that,

$$\mathbf{q}(i) = q(i) \mathbf{p}(i) \quad (11)$$

with  $q(i)$  being the modulus of  $\mathbf{q}(i)$ . Equation (5) becomes

$$\frac{d}{dt} \mathbf{q}(i) = \mathbf{L} \cdot \mathbf{q}(i) + q(i) \mathbf{F}^{(b)}(t). \quad (12)$$

Rewriting Eq.(12),

$$\frac{\partial}{\partial t} \mathbf{q}(i) = -\mathbf{u} \cdot \nabla \mathbf{q}(i) + \mathbf{L} \cdot \mathbf{q}(i) + q(i) \sqrt{2C_i \dot{\gamma}} \frac{d\mathbf{w}}{dt}. \quad (13)$$

This equation can be solved using the time marching scheme with the evolution of the flow field for each fibre at all the nodes.

### Level Set Method for Two-Phase Flows

The level set method is to solve the following convective equation,

$$\frac{\partial \phi}{\partial t} + \mathbf{u} \cdot \nabla \phi = 0, \quad (14)$$

where  $\phi$  is the level set function and  $\mathbf{u}$  is the ‘‘unified’’ fluid velocity. The interface between the two fluids is expressed by a zero value of a function  $\phi$ ; the function is positive in one phase and is negative in another phase. In the computing, the level set function is initialized as a signed distance function from the interface. Then, it is evolved according to Equation (14), which is solved by a time marching scheme. After each time step, the zero level set function should represent the position of the new interface. However, because of the numerical approximation, the level set function may not remain a distance function at later time steps; in particular after a long time. Therefore, it is suggested that the level set function is re-initialized after a time step so that it remains a distance function without changing its zero level set. Generally, this is achieved by solving the following partial differential equation [10,11],

$$\frac{\partial \phi}{\partial \tau} = \text{sign}(\phi)(1 - |\nabla \phi|) \quad (15)$$

with initial conditions

$$\phi(x,0) = \phi_0(x), \quad (16)$$

where  $\text{sign}(\phi)$  is a sign function, and  $\tau$  is the (artificial) time, and  $\phi_0(x)$  is the initial value of  $\phi$  given at the beginning of calculation for all of the domain.

The Navier-Stokes equations for two-fluid flows can be modified to include the surface tension force. Thus, the governing equation for the fluid velocity,  $\mathbf{u}$ , along with the boundary conditions can be combined in a single equation,

$$\rho(\phi) \frac{D\mathbf{u}}{Dt} = -\nabla p + \nabla \cdot \boldsymbol{\tau}_f + \mu(\phi) \nabla^2 \mathbf{u} + \rho(\phi) \mathbf{g} - \sigma k(\phi) \delta(\phi) \nabla \phi, \quad (17)$$

$$\nabla \cdot \mathbf{u} = 0,$$

where  $\rho(\phi)$  and  $\mu(\phi)$  are the density and viscosity, respectively, which are functions of  $\phi$ , and they are expressed by a smoothed heaviside function at the interface.  $\delta(\phi)$  is the Dirac delta function,  $\sigma$  is the surface tension factor, and  $k(\phi)$  is the curvature of the interface.

The equation (17) is rewritten as the dimensionless form,

$$\mathbf{u}_t + \frac{\nabla p}{\rho(\phi)} = \mathbf{F}, \quad (18)$$

where

$$\mathbf{F} = -\mathbf{u} \cdot \nabla \mathbf{u} - \frac{\mathbf{e}}{Fr} + \frac{1}{\rho(\phi)} \left( \frac{1}{\text{Re}} \nabla \cdot \boldsymbol{\tau}_f + \frac{1}{\text{Re}} \nabla \cdot (2\mu(\phi) \dot{\gamma}) - \frac{1}{We} k(\phi) \delta(\phi) \nabla \phi \right), \quad (19)$$

and  $\mathbf{e}$  is the unit vector of the gravitational force.

Sussman et al [11] described a variable density projection method. In this method, it is assumed that

$$\nabla \cdot \mathbf{u}_t = 0 \quad (20)$$

Thus, according to the Hodge decomposition, one can uniquely decompose the quantity  $\mathbf{F}$  found in Equation (18) into a divergence free part ( $\mathbf{u}_t$ ) and the gradient of a scalar divided by density ( $\nabla p / \rho(\phi)$ ). Since  $\mathbf{u}_t$  is divergence free we can write it as for two-dimensional flow,

$$\mathbf{u}_t = (\partial \psi_t / \partial y, \partial \psi_t / \partial x, 0)^T \quad (21)$$

where  $\psi_t$  is the stream function corresponding to  $\mathbf{u}_t$ .

For two-dimensional flows, if we multiply both sides of Equation (18) by  $\rho$  and take the curl of both sides, we then obtain,

$$-\nabla \cdot (\rho \nabla \psi_t) \mathbf{k} = \nabla \times (\rho \mathbf{F}), \quad (22)$$

where  $\mathbf{k}$  is the unit vector in the  $z$  direction.

For given smooth boundary conditions and initial conditions, Eq.(22) can be solved for the stream function for a prescribed time increment.

### Numerical Discretization and Algorithm

The discretization is based on a staggered grid arrangement, as shown in Fig. 1. Here,  $\mathbf{u}$ ,  $\mathbf{q}$ ,  $\rho$ ,  $\mu$ ,  $\phi$ , are given at the primary grid points denoted by open circles, and  $\psi_t$ ,  $\nabla \mathbf{u}$ , and  $\boldsymbol{\tau}$  are defined on the dual grid points denoted by ‘‘ $\times$ ’’. Actually, the dual grid points lie on the wall boundary of the physical domain for the imposition of the no-slip boundary conditions (Fig. 1). The numerical discretization has been described in [11-12].

The projection equation (22) is solved using a preconditioned conjugate gradient (PCG) method. Then,  $u_t$  is obtained by Eq.(21) using the central difference scheme. The

time marching of the dependent variable  $u$ ,  $v$ , and  $\phi$  are calculated by using a high order Total Variation Diminishing (TVD) Runge-Kutta scheme. The time step  $\Delta t$  is determined by restrictions due to CFL condition, gravity, viscosity and surface tension.

The total numerical procedure can be summarized as below:

- (1) Initialize all the parameters. Give initial  $\phi$  in the domain.
- (2) For given  $\phi^n$ ,  $\mathbf{u}^n$ ,  $\rho(\phi)$ ,  $\mu(\phi)$ , solve the Eq.(5) using the time march scheme, and obtain the fibre orientation distribution and the configuration tensor.
- (3) For given  $\phi^n$  and  $\mathbf{u}^n$ , calculate  $\rho(\phi)$  and  $\mu(\phi)$  etc., then calculate the convective term, viscous term and fibre stress term (Central difference), source term (coordinate components), and tension term in Eq.(19).
- (4) Solve equation (22) using a preconditioned conjugate gradient (PCG) method to get  $\psi_t$ . Calculate  $\mathbf{u}_t$  expressed by Eq.(21) by differencing  $\psi_t$ .
- (5) Determine the time step  $\Delta t$  using the criteria given; Do the time marching step for variables  $u$ ,  $v$ , and  $\phi$  using a high order total variation diminishing (TVD) Runge-Kutta scheme to obtain  $u^{n+1}$ ,  $v^{n+1}$ , and  $\phi^{n+1}$  (like  $\mathbf{u}^{n+1} = \mathbf{u}^n + \mathbf{u}_t \Delta t$ ).
- (6) Re-initialize the level set function for  $\phi^{n+1}$  following the equations (16).
- (7) Take the new  $u^{n+1}$ ,  $v^{n+1}$ , and  $\phi^{n+1}$  as the old ones, and then return to step (2).

### Simulation Results and Discussions

An annoying feature in the application of the projection/level set method is that it is required that the initial condition for the computational domain is divergence free. This requirement is only satisfied for few situations. Unfortunately, this condition is not satisfied for most open flow problems. In this study, first, we assign a continuous smooth distribution of stream function. Then, a divergence free velocity field is obtained from this stream function and is taken as the initial flow field.

The computing domain is shown in Fig.2 as a rectangular area with inlet AD, and BC the outlet. AB and CD are solid walls and EF is the interface of the two fluids. AB is taken as 4 times of AD, and AF is taken as 0.25 times of AD. The fluid flow is driven by a pressure gradient at the inlet in a two-dimensional channel. Initially, the fluid stays in the area enclosed by AFED. At time  $t=0$ , the fluid is allowed to flow as the given velocity distribution. At the first few steps, the flow will automatically adjust itself to obey the governing equations. After a long enough time and far enough from the inlet, the effect of initial flow field becomes small. The flow is dominated by the pressure gradient and viscous and fibre forces as well as the surface tension. For the laminar flow of a Newtonian fluid, it is thought that the velocity distribution in the duct far from the front obeys parabolic distribution, in which the effect of interface and surface tension can be neglected. In the simulation, we hope to track the evolution of the flow front, and to find the effect of fibre suspension properties. The boundary condition is taken such that AB and CD are solid surfaces and hence no-slip boundary condition applies. Boundary conditions at inlet for velocities are given at AD and Neumann boundary condition applies on BC. At the wall, the level set function is extrapolated to the wall from interior domain. The contact angle is not given as in most level set methods. The slope of the interface at the wall is directly obtained from the simulation. The BC on  $\mathbf{p}$  at the wall is given that the fibre is parallel to the wall ( $p_1=0$ ,  $p_2=1$ , and  $p_3=0$ ). The initial condition for  $\mathbf{p}$  within the domain is random (AFED in Fig.2). With the fluid flowing and the time involving, the orientation of the fibres will automatically adapt to the velocity

field. The simulation is carried out for given concentration and number of fibres. They are set to be constants in the domain as in [4,8]. Generally, there is no number limitation of fibres in principle, provided that the computer resources are sufficient large. Eq.(5) is solved for each fibre, and then assemble average is employed to calculate the stresses. Thus, it is better for the simulation to be carried out using a large number. However, the simulation results will be about the same when the number of fibres is larger than a sufficient large number. A large number for the fibres avoids the oscillation of the solutions. Numerical limitation is encountered when the concentration is high which leads to high stress gradients near the interface.

Simulation results for two examples are shown in Fig.3 and Fig.5 for Newtonian flow and fibre flow ( $\phi = 0.08$ ,  $a_r = 10$ ,  $\sigma = 0.01$ , and  $N=500$ ). The flow is from top to bottom. It can be seen that the addition of fibres makes the flow front more distorted. Compared to Newtonian flow, the presence of fibres affects the shapes of flow fronts and the flow front changes gradually with the increase of fibre concentration. The simulation results show that the fibres near the walls (high shear rate) generate high stresses, slow down the streamwise velocity, and increase the transverse velocity. This make the flow near the front form a fountain flow. Although the surface tension increases the strength of the "fountain," the primary reason of this front shape is due to the influence of fibre stresses. The velocity field is shown in Fig.3 and Fig.4 for Newtonian and fibre suspension cases. The difference is clearly demonstrated. The effect of fibres makes the front near the walls moving faster than that for Newtonian flow (Fig.5). After the flow evolving a long enough time, the flow front should approach steady-state geometries owing to the balance of various forces including surface tension. In Fig.5, the flow front is still under development at  $t=17$ .

Finally in conclusion, the front flow evolution in fibre suspension flows can be simulated with the projection scheme and the level set method. Using this algorithm, the effect of various material parameters on the flow properties and front shapes as well as the final fibre orientation can be obtained. This study will help to improve the product quality in injection moulding and other process industries.

### Acknowledgements

The authors are grateful to X-J Fan (The University of Sydney) for his helpful discussions and suggestions.

### References

1. Folgar, F.P. & Tucker, C.L., Orientation behavior of fibers in concentrated suspensions, *J. Reinforced Plastics and Composites*, 3, 1984, 98-119.
2. Advani, S.G. & Tucker, C.L., The use of tensors to describe and predict fibre orientation in short fibre composites, *J. of Rheol.*, 31, 1987, 751-784.
3. Phan-Thien, N. & Graham, A.L., A new constitutive model for fibre suspensions: flow past a sphere, *Rheol. Acta*, 30, 1991, 44-57.
4. Fan X.J., Phan-Thien, N. & Zheng R., Simulation of fibre suspension flows by the Brownian configuration field method, *J. Non-Newt. Fluid Mech.*, 84, 1999, 257-274.
5. Petrie, C.J.S., The rheology of fibre suspensions, *J. Non-Newt. Fluid Mech.*, 87, 1999, 369-402.
6. Baloch, A. & Webster, M.F., A computer-simulation of complex flows of fiber suspensions, *Comput. Fluids*, 24, 1995, 135-151.
7. Reddy, B.D. & Mitchell, G.P., Finite element analysis of fibre suspension flows, *Comput. Method Appl. Mech. & Eng.*, 190, 2001, 2349-2367.
8. Hulsen, M.A., van Heel, A.P.G. & van den Brule, B.H.A.A., Simulation of viscoelastic flows using Brownian configuration fields, *J. non-Newt. Fluid Mech.*, 70, 1997, 79-101.

9. Azaiez, J. & Guette, R., Numerical Modelling of the Flow of Fibre Suspensions through a Planar Contraction, *Canadian J of Chem. Engineering*, 80, 2002, 1115-1125.
10. Sethian, J.A. & Smereka, P., Level set methods for fluid interfaces, *Annu. Rev. Fluid Mech.*, 35, 2003, 341-372.
11. Sussman, M., Fatemi, E., Smereka, P. & Osher, S., An improved level set method of incompressible two-fluid flows, *Comput. Fluids*, 27, 1998, 663-680.
12. Dou, H.-S., Phan-thien, N., Khoo, B.C., Yeo, K.S. & Zheng, R., Simulation of front evolving liquid film flowing down an inclined plate using level set method, *Comput. Mech.*, 34, 2004, 271-281.
13. Jeffery, G.B., The motion of ellipsoidal particles immersed in viscous fluid, *Proc. Roy Soc. Lond.*, A102, 1922, 161-179.
14. Phan-Thien, N., Fan, X.J., Tanner, R.I. & Zheng, R., Folgar-Tucker constant for a fibre suspension in a Newtonian fluid, *J. Non-Newt. Fluid Mech.*, 103, 2002, 251-260.

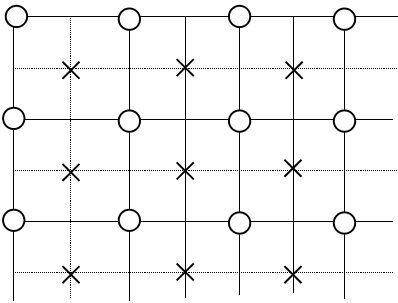


**Fig.1.** Schematic of the grid arrangement. Primary grid points O: for  $\mathbf{u}$ ,  $\mathbf{q}$ ,  $\rho$ ,  $\mu$ ,  $\phi$ ; Dual grid points  $\times$ : for  $\psi_t$ ,  $\nabla \mathbf{u}$ ,  $\boldsymbol{\tau}$ , and the resulting  $p$ .

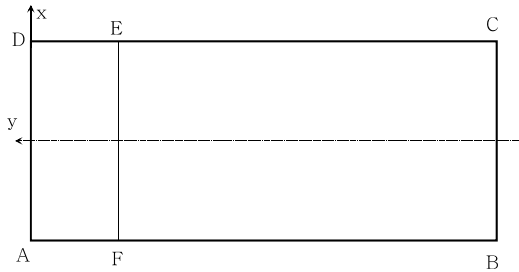


**Fig.2.** Schematic of the computing domain

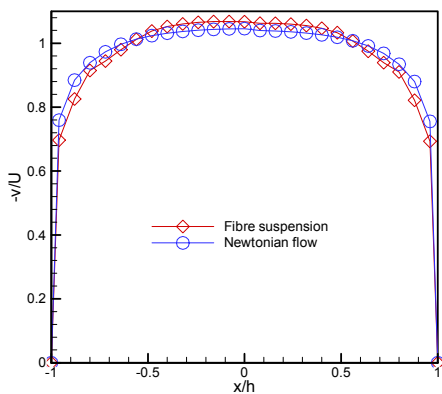


**Fig.3** Streamwise velocity profile at the position just behind the front for  $t=15$ .

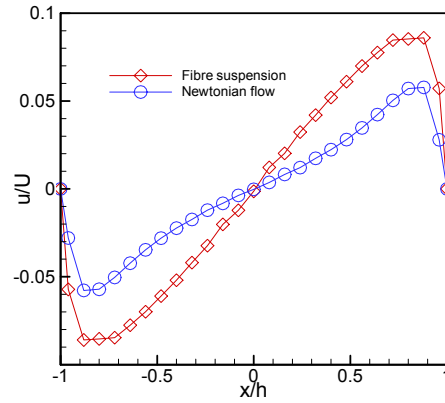


**Fig.4.** Velocity profile in transverse direction at the position just behind the front for  $t=15$ .

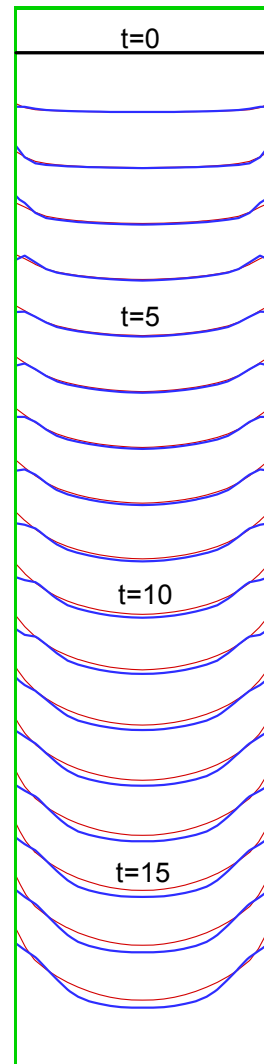


**Fig.5** Computing results for the flow front evolution for Newtonian flow (red thin line) and fibre suspension flow (blue thick line,  $\phi = 0.08$ ,  $a_r = 10$ ,  $N = 500$ ,  $C_i = 0.01$ ). Reynolds number is 60 based on the viscosity of the solvent; Grid is  $271 \times 100$ ; Time interval of the front contact  $\Delta t = 0.01$  second. Surface tensor coefficient is  $\sigma = 0.01$  N/m.